VME-DWT: An Efficient Algorithm for Detection and Elimination of Eye Blink From Short Segments of Single EEG Channel

Mohammad Shahbakhti, Matin Beiramvand, Mojtaba Nazari, Anna Broniec-Wójcik, Piotr Augustyniak, *Senior Member, IEEE*, Ana Santos Rodrigues, Michal Wierzchon, and Vaidotas Marozas, *Member, IEEE*

***Abstract*— *Objective*: Recent advances in development of low-cost single-channel electroencephalography (EEG) headbands have opened new possibilities for applications in health monitoring and brain-computer interface (BCI) systems. These recorded EEG signals, however, are often contaminated by eye blink artifacts that can yield the fallacious interpretation of the brain activity. This paper proposes an efficient algorithm, VME-DWT, to remove eye blinks in a short segment of the single EEG channel. *Method*: The proposed algorithm: (a) locates eye blink intervals using Variational Mode Extraction (VME) and (b) filters only contaminated EEG interval using an automatic Discrete Wavelet Transform (DWT) algorithm. The performance of VME-DWT is compared with an automatic Variational Mode Decomposition (AVMD) and a DWT-based algorithms, proposed for suppressing eye blinks in a short segment of the single EEG channel. *Results*: The VME-DWT detects and filters 95% of the eye blinks from the contaminated EEG signals with SNR ranging from −8 to +3 dB. The VME-DWT shows superiority to the AVMD and DWT with the higher mean value of correlation coefficient (0.92 vs. 0.83, 0.58) and lower mean value of RRMSE (0.42 vs. 0.59, 0.87). *Significance*: The VME-DWT can be a suitable algorithm for removal of eye blinks in low-cost single-channel EEG systems as it is: (a) computationally-efficient, the contaminated EEG signal is filtered in millisecond time resolution, (b) automatic, no human intervention is required, (c) low-invasive, EEG intervals without contamination remained unaltered, and (d) low-complexity, without need to the artifact reference.**

***Index Terms*— EEG, denoising, eye blink, VME, DWT.**

Manuscript received November 10, 2020; revised January 6, 2021; accepted January 22, 2021. Date of publication January 26, 2021; date of current version March 2, 2021. *(Corresponding author: Mohammad Shahbakhti.)*

Mohammad Shahbakhti, Ana Santos Rodrigues, and Vaidotas Marozas are with the Biomedical Engineering Institute, Kaunas University of Technology, 44249 Kaunas, Lithuania (e-mail: mohammad.shahbakhti@ktu.edu).

Matin Beiramvand is with the Department of Biomedical Engineering, Dezful Branch, Islamic Azad University, Dezful 6468118333, Iran.

Mojtaba Nazari is with the Department of Electrical and Computer Engineering, Babol Noshirvani University of Technology, Babol 47148-71167, Iran.

Anna Broniec-Wójcik and Piotr Augustyniak are with the Department of Biocybernetics and Biomedical Engineering, AGH University of Science and Technology, 30-059 Kraków, Poland.

Michal Wierzchon is with the Institute of Psychology, Jagiellonian University, 31-007 Kraków, Poland.

Digital Object Identifier 10.1109/TNSRE.2021.3054733

I. Introduction

THE advent of portable single-channel electroencephalography (EEG) has been transforming health monitoring and brain-computer interfacing (BCI), particularly for indoor and non-clinical environments. Prefrontal single-channel EEG systems can be more convenient for the long-term monitoring [1], [2] and have been employed successfully in various applications [3]–[8]. Unfortunately, EEG signals are highly susceptible to artifacts incited by numerous sources, either non-physiological (e.g., power line interference and electrode pop), or physiological (e.g., cardiac and muscular contractions) [9], [10]. Among the latter are eye blink artifacts, which are prominent in frontal channels [11] due to its amplitude and frequency range. Eye blinks are involuntary and, thus, unavoidable in long-term monitoring [12]. One possible solution is to record EEG with eyes-closed, however, such a strategy can yield the undesirable alternation of EEG rhythms [13] and evidently is not applicable in experiments with visual stimulation. As with any artifact, the filtering of eye blinks in EEG signals is crucial before further processing to avoid an erroneous brain activity analysis [12]. While numerous algorithms are available for multi-channel and offline eye blink filtering [14]–[16], unsupervised low-complexity algorithms capable of removing eye blinks in a short segment of a single-channel EEG for real and semi-real time applications are still lacking.

Subtraction, regression, and adaptive filters are amongst the most straightforward strategy for eye blink removal in the single EEG channel. However, such filters require the artifact reference channel, thus increasing hardware complexity, which is disadvantageous for low-cost EEG headbands. Additionally, algorithms based on such filters presume that no bidirectional contamination exists between the recorded artifact reference and desired EEG, which is not always correct [11]. Wiener filters could combat the need for an extra artifact reference channel but with the drawback of requiring initial calibration [17].

Signal decomposition algorithms such as wavelet [18]–[20], Empirical Mode Decomposition (EMD) [21], and Variational Mode Decomposition (VMD) [22] require neither the artifact reference channel nor the initial calibration. Indeed, an automatic algorithm based on VMD and linear

regression (AVMD) [23] was proposed for the removal of eye blinks in a short segments of single-channel EEG, outperforming EMD, ensemble EMD (EEMD), Independent Component Analysis (ICA), and wavelet enhanced ICA algorithms. A common problem of signal decomposition-based algorithms is the inability to limit filtering to the actual artifactual eye blink interval, typically 200-400 ms long [9]. Instead, such algorithms filter the whole segment of the contaminated EEG signal, e.g., 3s, which can eliminate some of the non-artifactual components of EEG signals. Thus, algorithms capable of restricting filtering to the artifactual intervals without compromising the desired EEG components are needed.

Restricting filtering to the artifactual eye blink interval could be accomplished using artifact detection strategies, such as amplitude thresholding, derivatives, or template matching. Amplitude threshold-based algorithms show limitations when other high amplitude artifacts appear [24]. Moreover, eye blinks with an amplitude lower than the threshold cannot be detected [25]. Derivative-based algorithms detect sudden changes by presuming that a triangular-shape morphology represents an eye blink event [26], which is a controversial presumption [27]. Lastly, template matching algorithms employ a threshold to assess the similarity between EEG segments and a provided template. Thus, the success of template matching algorithms depends on correctly defining both the template and threshold value. The iterative template matching and suppression (ITMS) algorithm [27] was proposed to detect and eliminate eye blinks from a single-channel EEG with an automatic threshold and template estimation. Despite the excellent performance, the ITMS algorithm is only applicable for offline processing since it requires a sufficient number of eye blink events for an accurate filtering. In specific portable-EEG applications, real-time removal of eye blinks is crucial, meaning that algorithms must filter the artifactual intervals in short segments.

This paper presents an efficient algorithm, VME-DWT, for the unsupervised detection and filtering of eye blinks in a short segment (i.e., 3s) of a single-channel EEG without the mentioned limitations. The artifactual eye blink intervals are detected using Variational Mode Extraction (VME) [28], followed by an automatic Discrete Wavelet Transform (DWT) to filter the contaminated intervals. VME extracts an approximation of the eye blink signal from the contaminated EEG, facilitating the search for eye blink peak to form the artifactual interval. DWT then only filters the selected interval, preserving the non-artifactual intervals of EEG signals, without requiring any prior calibration or artifact reference. The performance of VME-DWT are investigated on both semi-simulated and real contaminated EEG data and then compared to the AVMD [23] and DWT [19] algorithms, which, as mentioned above, have been developed for the eye blink filtering in a short segments of the single-channel EEG.

II. Materials and Methods

A. VME Algorithm

VMD has been introduced as a tool to decompose a non-stationary signal, $x(n)$, into K number of modes, $u_k(n)$, called band limited intrinsic mode functions (BLIMFs) subject to $x(n) = \sum_{k=1}^{K} u_k(n)$ [29]. Each mode of VMD is centered around a center frequency, ω_k.

The objective of VMD is to extract all possible modes from the input signal, that might yield unnecessary computational burdens, and is not required in some application, e.g., artifact detection. To this end, a simplified version of VMD, called VME, has been introduced to extract a desired mode from the input signal by having an approximate value of the center frequency. The basis of VME is to decompose the input signal $x(n)$ into a desired mode, $u_d(n)$ with a pre-defined center frequency, ω_d and a residual signal $x_r(n)$ such as $x(n) = u_d(n) + x_r(n)$.

The desired mode is computed by its bandwidth minimization around its center frequency. The VME models the bandwidth of desired mode with the following steps:

1. For the given mode of interest $u_d(n)$, the analytic signal is computed using Hilbert transform as $[(\delta(n) + \frac{j}{n\pi}) * u_d(n)]$, where $\delta(n)$ is the Dirac distribution and * denotes convolution.
2. The frequency of the analytical signal is shifted to the center frequency by its multiplication to an exponential ω_d tuned as $[(\delta(n) + \frac{j}{n\pi}) * u_d(n)]e^{-j\omega_d n}$.
3. The gradient of the second norm squared of the shifted analytical signal is considered as the bandwidth.

In order to VME successfully extracts the desired mode $u_d(n)$ with the center frequency of ω_d, the following conditions must be fulfilled:

1. The mode of interest $u_d(n)$ must be compacted around ω_d. As a result, the following bandwidth must be minimized:

$$J_1 = \left\| \partial_n \left[(\delta(n) + \frac{j}{n\pi}) * u_d(n) \right] e^{-j\omega_d n} \right\|_2^2 \tag{1}$$

2. The spectral overlap of the residual signal $x_r(n)$ and the desired mode $u_d(n)$ should be minimized to guarantee the fully extracted mode. Therefore, a filter is required to properly separate the component which lie in the frequency range of the desired mode. To this aim, the following filter is used:

$$\beta(\omega) = \frac{1}{\alpha(\omega - \omega_d)^2} \tag{2}$$

where α regulates the bandwidth of filter. According to equation (2), infinite sensitivity is achieved at $\omega = \omega_d$. As a result, minimization of the spectral overlapping of the $x_r(n)$ and $u_d(n)$ can be solved by following penalty equation:

$$J_2 = \|\beta(n) * x_r(n)\|_2^2 \tag{3}$$

where $\beta(n)$ is the impulse response of the filter.

The desired mode should be such that the original signal can be reconstructed by the summation of residual signal and the extracted desired mode. Hence, the problem of desired mode extraction can be solved by the constrained minimization of following criterion:

$$\min_{u_d, \omega_d, x_r} \{\alpha J_1 + J_2\}, \quad \text{s.t.} : u_d(n) + x_r(n) = x(n) \tag{4}$$

In order to render the unconstraintity of equation (4), a quadratic penalty term and a Lagrange multiplier can be

applied as follows:

$$\begin{aligned}&\mathcal{L}(u_d, \omega_d, x_r, \lambda)\\ &:= \alpha \left\| \partial_n \left[(\delta_n + \frac{j}{n\pi}) * u_d(n) \right] e^{-j\omega_d n} \right\|_2^2\\ &\quad + \|\beta(n) * x_r(n)\|_2^2 + \|x(n) - [u_d(n) + x_r(n)]\|_2^2\\ &\quad + \langle \lambda(n), x(n) - [u_d(n) + x_r(n)] \rangle \end{aligned} \tag{5}$$

where λ expresses the Lagrange multiplier. The saddle point of equation (5), that corresponds to the solution of equation (4), can be estimated by alternate direction method of multipliers (ADMM). Taking into account the ADMM is an iterative algorithm, Parseval's equality and simplifying some mathematical expressions, the desired mode $u_d(n)$, center frequency ω_d and Lagrange multiplier λ are updated at each iteration of m as follows:

Algorithm 1 VME Algorithm, Adapted From [28]

Input: Signal $x(n)$, α, and ω_d

Output: The desired mode $u_d(n)$

Initialisation $\hat{u}_d^1(n)$, $\hat{\lambda}^1$, $m \leftarrow 0$

Repeat $m \leftarrow m + 1$

1: Update $\hat{u}_d$ for $\omega \geqslant 0$

$$\hat{u}_d^{m+1}(\omega) \leftarrow \frac{\hat{x}(\omega) + \alpha^2(\omega - \omega_d^m)^4 \hat{u}_d^m(\omega) + \frac{\hat{\lambda}(\omega)}{2}}{[1+\alpha^2(\omega-\omega_d^m)^4][1+2\alpha(\omega-\omega_d^m)^2]}$$

2: Update ω_d

$$\omega_d^{m+1} \leftarrow \frac{\sum_0^\infty \omega |\hat{u}_d^{m+1}(\omega)|^2}{\sum_0^\infty |\hat{u}_d^{m+1}(\omega)|^2}$$

3: Dual Ascent for all $\omega \geqslant 0$

$$\hat{\lambda}^{m+1}(\omega) \leftarrow \hat{\lambda}^m(\omega) + \tau\left[\hat{x}(\omega) - \left(\hat{u}_d^{m+1}(\omega) + \hat{x}_r(\omega)\right)\right]$$

4: Until the convergence:

$$\frac{\left\|\hat{u}_d^{m+1} - \hat{u}_d^m\right\|_2^2}{\|\hat{u}_d^m\|_2^2} < \epsilon$$

For more details, readers are encouraged to see [28].

B. The VME-DWT Algorithm

The VME firstly extracts an approximation of the eye blink signal to localize the highest eye blink peaks, and detects the artifactual intervals containing eye blinks. Then identified intervals are filtered using DWT, maximizing the preservation of eye blink-free EEG. The block diagram of the proposed algorithm is shown in Fig.1.[1]

1) Eye Blink Detection Using VME: The VME algorithm requires two parameters to be set: the compactness coefficient α and the approximate value of center frequency ω_d of the desired mode. Although the authors in [28] recommend high α values to ensure the detected center frequency is related to the desired mode, smaller α values are better suited to extract all eye blink-related components due to the eye blink frequency range (0.5-7.5 Hz) and its spectral overlapping in EEG signals. To find the best α fit, we initialize α at 7000, decreasing with a 1000-step until 2000. The approximate center frequency is selected based on the eye blink frequency to a value of 3 Hz.

[1]The MATLAB code is available on GitHub with repository name: VMEDWT-Eyeblink-Elimination

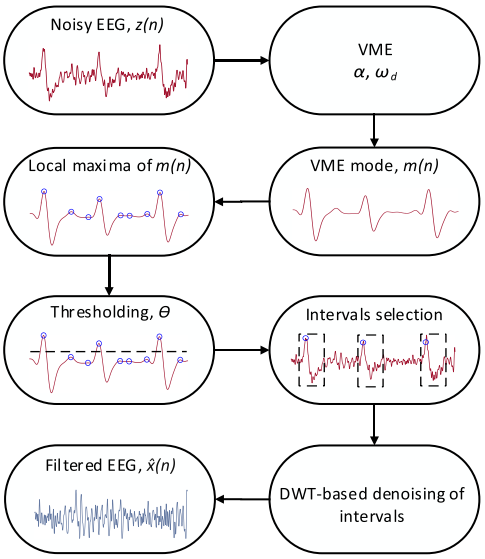

Fig. 1. The block diagram of the proposed algorithm.

After extracting the desired mode, $m(n)$, the eye blinks peaks are located by computing the local maxima of $m(n)$ that have values greater than the universal threshold [16], [20], [30] expressed as follows:

$$\theta = \frac{\text{median}(|m(n)|)}{0.6745}\sqrt{2\log N} \tag{6}$$

where $m(n)$ is the desired mode extracted by VME and N is the signal length in samples. After localizing every eye blink's highest peak in $m(n)$, they will be projected to contaminated EEG to set intervals for the time-selective filtering of eye blink components. Since the eye blink duration varies from 200 to 400 ms [9], [30]–[32], a 500 ms interval (125 ms pre- and 375 ms post the highest amplitude peak) is chosen to ensure all eye blink components are included even if the algorithm does not precisely localize the highest eye blink peak.

2) Double Eye Blink: In some cases, two eye blink events might overlap. While the proposed algorithm can detect them, the filtering is performed twice, increasing computational complexity and yielding extra data loss. To overcome this issue, a simple criterion that measures the distance between the identified eye blink peaks is employed. If the distance between two eye blink peaks is smaller than 500 ms, the artifactual window is updated to 125 ms pre-first highest eye blink peak and 375 ms post second highest eye blink peak (Fig. 2).

3) Eye Blink Filtering Using DWT: DWT decomposes an input signal $x(n)$ into low and high frequency components known as approximation $a(n)$ and detail components $d(n)$, respectively. The original input signal can be reconstructed entirely by $x(n) = \sum_{l=1}^{L} d_l(n) + a_L(n)$, where L is the number of decomposition level.

DWT requires two parameters to be set: the mother wavelet and the decomposition level. Analogously to previous studies [33], [34], db4 is selected as the mother wavelet as its morphology resembles that of eye blinks. The selection of decomposition level is a more painstaking task as EEG signals from different databases might require distinctive number of

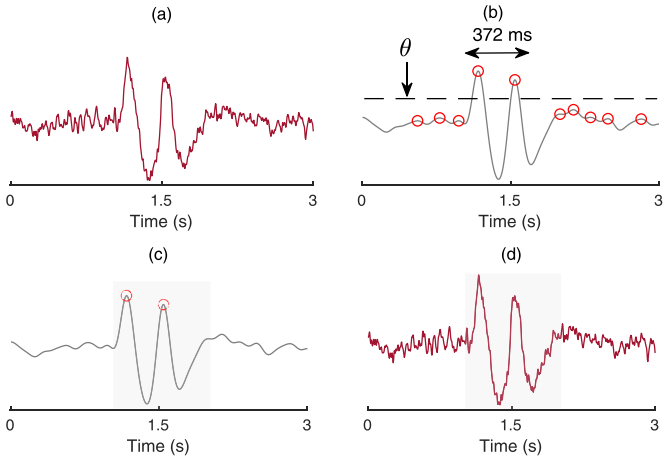

Fig. 2. Examples of a contaminated EEG with a double eye blink (a), extracted VME mode with detected eye blink peaks (b), formed the artifactual window on VME mode (c), and EEG with projected the artifactual interval (d).

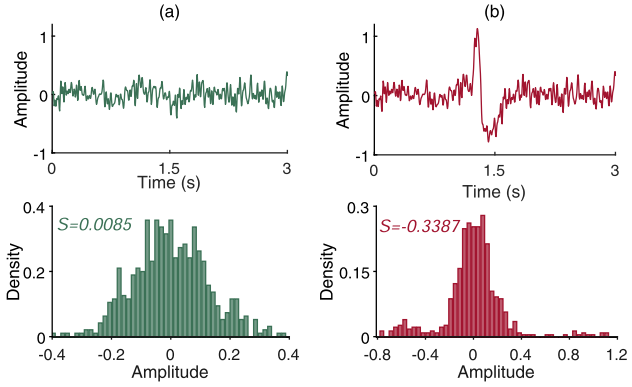

Fig. 3. Examples of eye blink-free (a) and contaminated (b) EEG signals with the corresponding distributions. *S* indicates the skewness value.

decomposition levels for denoising [20], [34]–[36]. The most straightforward strategy is to employ full tree decomposition, however, such a strategy may increase unnecessary computational requirements. To this end, we use a skewness-based strategy to control and find the best decomposition level. Since the eye blink amplitude is significantly higher than the EEG signal, its emergence can lead to an asymmetric distribution of the EEG signal [10], [21], [37]. Thus, large absolute skewness values in DWT components can indicate eye blink existence (Fig. 3). Compared to EEG signal, eye blink is a low-frequency phenomenon. Thus, its components are expected to emerge in the approximations $a(n)$ of the decomposed signal. The absolute difference of skewness values at two consecutive approximation components is, therefore, used as the decisive factor whether to terminate or continue the decomposition process:

$$\delta = \left||S_j| - |S_{j-1}|\right| \tag{7}$$

where S is the skewness and j is the level of decomposition. If $\delta > T$, it can be assumed that DWT has reached the blink components. The threshold value, T is tuned based on the lowest error between the eye blink-free and filtered EEG signals.

The main steps of proposed VME-DWT are summarized in Algorithm 2.

Algorithm 2 VME-DWT for Eye Blink Removal

Input: Noisy EEG $z(n)$, α, ω_d, Fs, T
Output: Filtered EEG $\hat{x}(n)$
Initialisation $\theta, \delta \leftarrow 0$, $j \leftarrow 2$
{*Detect Artifactual Interval*}
$m(n) \leftarrow$VME$(z(n), \alpha, \omega_d)$
$\theta \leftarrow$ see equation (6)
for $i = 2$ to $3 * Fs - 1$ **do**
  if $m(i) > m(i-1)$ && $m(i) > m(i+1)$ && $m(i) > \theta$ **then**
    $onset \leftarrow i - 0.125 \times Fs$
    $offset \leftarrow i + 0.375 \times Fs$
    $z_1(n) \leftarrow z(onset{:}offset)$
  end if
end for
{*Filter Artifactual Interval*}
while true **do**
  $a_{j-1}(n) \leftarrow$DWT$(z_1(n), j-1)$
  $a_j(n) \leftarrow$DWT$(z_1(n), j)$
  $S_{j-1} \leftarrow$skewness$(a_{j-1}(n))$
  $S_j \leftarrow$skewness$(a_j(n))$
  $\delta \leftarrow \left||S_j| - |S_{j-1}|\right|$
  if $\delta > T$ **then**
    Remove $a_j(n)$
    $\hat{x}(n) \leftarrow$ Reconstruct filtered EEG by summation of $d_1(n), .., dj(n)$
    break
  else
    $j \leftarrow j + 1$
  end if
end while
return $\hat{x}(n)$

C. Data

Semi-simulated and real eye blink-contaminated EEG signals have been used to develop and test the algorithm.

1) Semi-Simulated Data: To generate semi-simulated data, synthetic eye blink signals have been produced by repeating an eye blink template from [27] with different amplitudes at random time intervals. The generated eye blinks have been added to 1368 three-second long artifact-free EEG segments collected from [38]. The EEG signals were recorded according to the International System 10-20 with a sampling frequency of 200 Hz. EEG data were carefully captured to minimize the appearance of the external and physiological artifacts. A random noise is also added to our semi-simulated data to resemble real world EEG data better:

$$z(n) = x(n) + r(n) + v(n) \tag{8}$$

where $z(n)$ is the noisy EEG, $x(n)$ is the artifact-free EEG, $r(n)$ is the eye blink artifact and $v(n)$ is the noise that might

TABLE I
BRIEF DESCRIPTION OF THE EMPLOYED DATABASES FOR REAL EEG DATA ANALYSIS

Database	[39]	[40]	[41]	[42]
Sampling rate (Hz)	512	200	256	250
Electrode montage	10-10	10-20	10-10	10-20
No. of used subjects	4	6	7	15
No. used signals	444	1036	724	796

emerge in EEG signals from other sources such as environment or muscle contractions. Accordingly, we generated contaminated EEG signals with different Signal-to-Noise Ratio (SNR) values.

2) Real Data: The performance of all algorithms is tested on real data comprised of 3000 three-second long EEG segments from frontal channels, drawn from four BCI public databases [39]–[42]. Table I displays the information about each database.

The motivation behind using different databases is to investigate the adaptiveness of the proposed algorithm's parameters for EEG signals recorded in different conditions. These databases were purposely selected due to their realistic signal acquisition conditions as no artifact control or rejection was employed during recording. For more details about the data, see [39]–[42].

D. Algorithm Under Comparison

To compare the performance and computational complexity of the proposed algorithm, AVMD and DWT algorithms, proposed for eye blink filtering in a short segment of single-channel EEG, is used.

1) AVMD: The key steps of AVMD is to (i) decompose the contaminated EEG signal into 12 modes by VMD, (ii) find the artifactual modes based on amplitude and frequency thresholds, (iii) employ the summation of the artifactual modes as the input of linear regression to estimate the eye blink in the contaminated EEG signals, and (iv) subtract the estimated eye blink from the contaminated EEG signal. The required parameters of AVMD have been set as described in [23].

2) DWT: The basis of DWT denoising algorithm is to (i) decompose the input signal into l levels of coefficients using a basis function, (ii) set the coefficients of each level with a higher value than the threshold to zero, and (iii) reconstruct the denoised signal with inverse DWT. In [19], four basic functions, $haar$, $coif3$, $sym3$, and $bior4.4$ with universal and statistical thresholding have been investigated. According to the authors, $bior4.4$ basis function with the statistical thresholding can be the optimal choice for eye blink removal.

E. Evaluation Criteria

1) Eye Blink Detection: To assess the accuracy of eye blink detection, true positive rate (TPR) and false positive rate per interval (FPR) are computed as follows:

$$\mathrm{TPR} = \frac{\mathrm{TP}}{\mathrm{TP} + \mathrm{FN}} \tag{9}$$

$$\mathrm{FPR} = \frac{\mathrm{FP}}{\mathrm{FP} + \mathrm{TN}} \tag{10}$$

where TP (true positive), FN (false negative) and FP (false positive) stand for the correct, missed and false number of detected eye blinks, respectively. It should be noted that TN (true negative) concept does not exists in the continuous signal, therefore, FPR is assessed over the time intervals [27].

2) Filtering Performance: The filtering performance of the VME-DWT and AVMD algorithms is evaluated in both time and frequency domains. Regarding the time domain, the correlation coefficient (CC) and relative root mean square error (RRMSE) are computed between the eye blink-free and filtered EEG signals. The CC is expressed as

$$\mathrm{CC} = \frac{\mathrm{cov}\big(x(n), \hat{x}(n)\big)}{\sigma_{x(n)}\sigma_{\hat{x}(n)}} \tag{11}$$

where cov and σ are the covariance and standard deviation, $x(n)$ and $\hat{x}(n)$ are the eye blink-free and filtered EEG signals, respectively. The CC investigates the degree of linear dependence between two signals and varies from -1 to 1, where CC values closer to 1 indicates better quality of the filtering.

The RRMSE measures the amplitude distortion of the filtered EEG signals as follows:

$$\mathrm{RRMSE} = \frac{\mathrm{RMS}\big(x(n) - \hat{x}(n)\big)}{\mathrm{RMS}\big(x(n)\big)} \tag{12}$$

Lower RRMSE values indicate better filtering quality.

The difference of power spectral density (PSD) between the corresponding EEG bands (as described in [10]) of filtered and eye blink-free signals are used to evaluate the preservation of the frequency components, and it is computed as follows [23]:

$$\Delta\mathrm{PSD}_b = \mathrm{PSD}_b^{\text{eye blink-free EEG}} - \mathrm{PSD}_b^{\text{filtered EEG}} \tag{13}$$

where b indicates the band of EEG. Lower values of ΔPSD indicate better quality for preservation of the frequency component.

F. Optimization of VME-DWT Parameters

The optimization of the proposed algorithm's required parameters is conducted using 456 segments of the semi-simulated data. The α value, which plays the most important role for eye blink detection, is adjusted based on the highest mean of TPR and the lowest mean of FPR in the contaminated EEG signals with different SNR values. Fig. 4 confirms that the optimum α value is 3000.

As for T, which controls the DWT decomposition level, it is tuned based on the highest and lowest mean of CC and RRMSE, respectively, between the filtered and eye blink-free EEG signals. T values ranging from 0.05 to 0.25 with a step of 0.05 are employed. Fig. 5 shows that the optimum T value is 0.1.

Note that these 456 signals were only used for the optimization of VME-DWT algorithm and are not included for

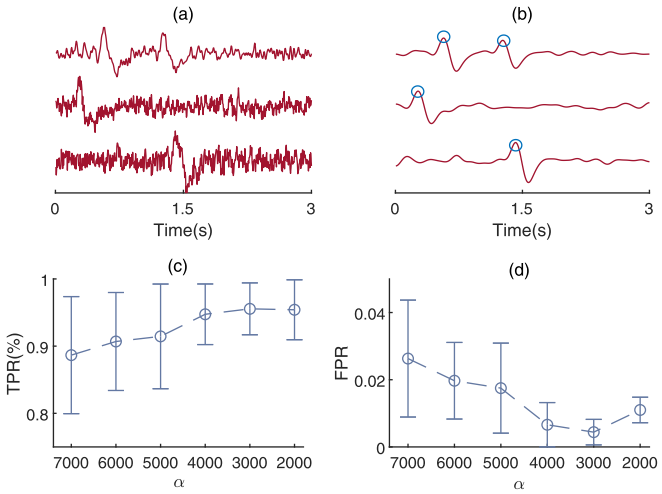

Fig. 4. Examples of contaminated EEG signals with different SNRs **(a)**, the corresponding desired mode extracted by VME **(b)**, the true positive rate **(c)**, and false positive rate per interval **(d)**.

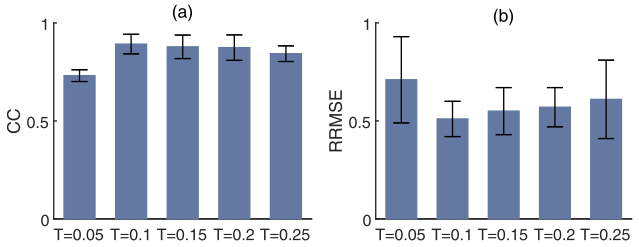

Fig. 5. The mean±SD of CC **(a)** and RRMSE **(b)** between the eye blink-free and filtered EEG signals.

TABLE II
PERCENTAGE OF TPR AND FPR OF VME-DWT FOR EYE BLINK DETECTION

SNR(dB)	TPR(%)	FPR
SNR$\geq$ 0	99.54	0.0004
-6<SNR<0	96.45	0.0032
SNR≤ -6	91.34	0.0136
Mean±SD	95.77±4.14	0.0057±0.007

the performance evaluation. The rest of semi-simulated data and four real EEG databases are filtered with $\alpha = 3000$ and $T = 0.1$ values to investigate their adaptivness for different EEG databases.

III. RESULTS

A. Filtering Results for Semi-Simulated Data

Table II discloses TPR and FPR values for eye blink detection in 912 three-second long segments of contaminated EEG signals with SNR ranging from -8 to $+3$ dB. The VME-DWT detected, on average, more than 95% of the eye blinks with an α value of 3000 for all SNRs.

Fig. 6 shows examples of the contaminated and their corresponding eye blink-free and filtered EEG signals with

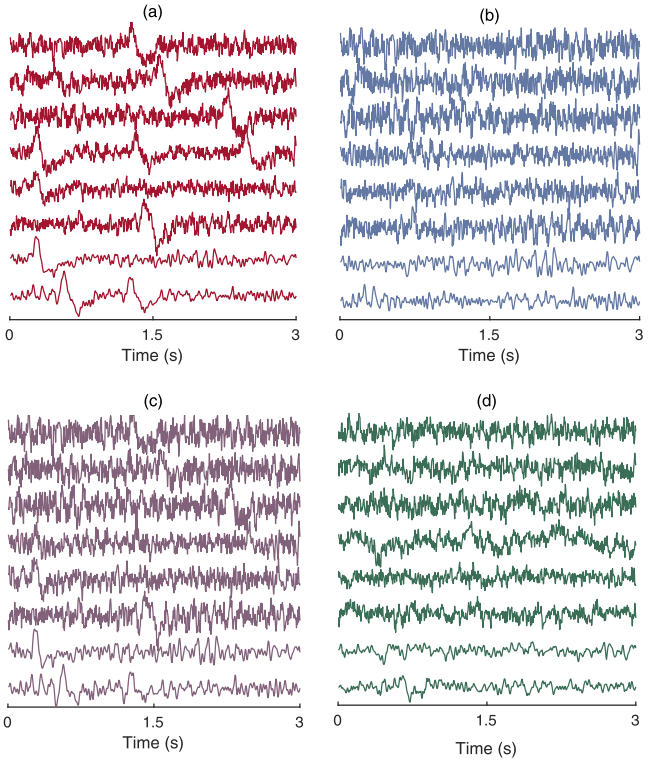

Fig. 6. Examples of contaminated **(a)**, eye blink-free **(b)** and filtered EEG signals by the VME-DWT **(c)**, and AVMD **(d)** algorithms.

different SNRs. In terms of the visual inspection, the VME-DWT eliminated eye blinks components better than the AVMD and DWT.

The boxplots of the CC and RRMSE values between the eye blink-free and filtered EEG signals are shown in Fig. 7. Compared to the AVMD and DWT, the VME-DWT displays lower mean value of RRMSE (0.42 vs. 0.59, 0.87) and higher CC mean value (0.92 vs. 0.83, 0.58), indicating that the proposed VME-DWT can better preserve the original eye blink-free EEG signals.

To assess the reliability of both algorithms at different SNR values, the CC and RRMSE as a function of SNR values are shown in Fig. 8. As it is observable, the proposed VME-DWT is more robust for different SNR values compared to the AVMD and DWT.[2]

Fig. 9 illustrates two examples of the PSDs between the eye blink-free and filtered EEG signals by all algorithms. The spectral analysis suggests that the proposed VME-DWT retains low-frequency components, thus better preserving the natural frequency spectrum of the artifact-fee EEG signals. Indeed, VME-DWT outperforms AVMD and DWT by better preserving delta, theta, alpha, and gamma bands, as disclosed in Table III. However, all algorithms show undesirably high ΔPSD values for the beta band.

B. Filtering Results for Real Data

Table IV displays the TRP(%) and FPR for eye blink detection in all four real EEG databases. As it is shown,

[2]Non-integer SNR values have been rounded

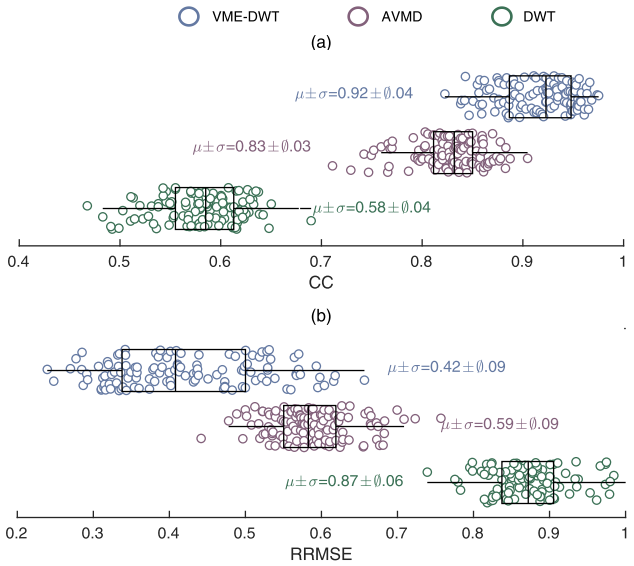

Fig. 7. Boxplots of CC **(a)** and RRMSE **(b)** between the eye blink-free and filtered EEG signals for all algorithms. μ and σ stand for mean and standard deviation.

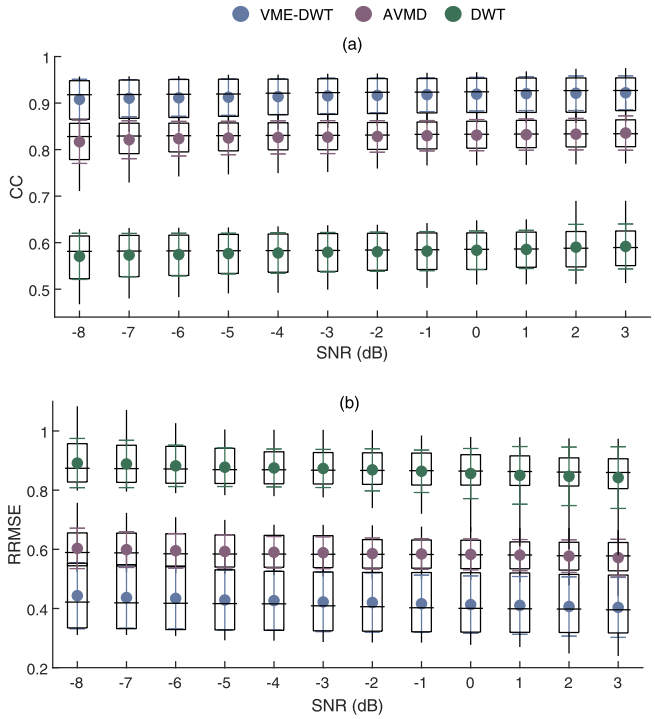

Fig. 8. The CC **(a)** and RRMSE **(b)** measures as a function of SNR for the filtered EEG signals by the proposed VME-DWT, AVMD and DWT algorithms.

the proposed algorithm could detect majority of the eye blink artifacts in EEG signals captured with distinctive recording conditions. It should be noted that due to unavailability of the artifact-free EEG, the computation of TPR and FPR for different SNRs is not possible.

Fig. 10 depicts examples of real contaminated EEG signals from all four databases with their corresponding filtered EEG signals. As it can be observed, the proposed algorithm can significantly better filter the intervals with eye blink artifacts.

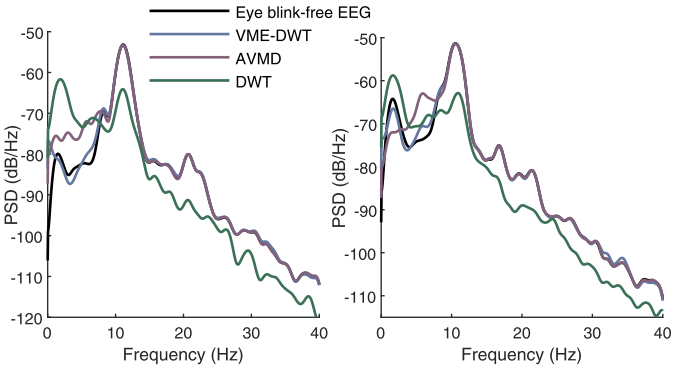

Fig. 9. Two examples of the spectral analysis between the eye blink-free and corresponding filtered EEG signals.

TABLE III
ΔPSD (MEAN±SD) FOR EEG BANDS AFTER FILTERING

EEG bands	VME-DWT	AVMD	DWT
Gamma	1.90±1.01	2.01±1.08	3.23±1.59
Beta	6.02±2.73	5.39±2.61	7.10±1.41
Alpha	1.39±0.81	2.30±1.60	2.94±1.72
Theta	3.98±1.71	5.19±2.78	7.39±2.61
Delta	4.58±1.93	8.53±3.73	10.48±3.53

TABLE IV
PERCENTAGE OF TPR AND FPR OF VME-DWT FOR EYE BLINK DETECTION IN FOUR REAL EEG DATABASES

Database	[39]	[40]	[41]	[42]
TPR(%)	95.24	94.12	93.32	98.52
FPR	0.0042	0.0071	0.0098	0.0083

Because the real artifact-free EEG signals are unknown, the temporal criteria were only computed between the eye blink-free intervals of real and filtered EEG signals [17]. Table V suggests superiority of the VME-DWT to the AVMD and DWT for the preservation of non-artifactual intervals.

C. Computational Complexity

Besides the performance, computational complexity of the denoising algorithms is another important factor that should be considered for real or semi-real time procedures. Taking into account that recursive Fast Fourier Transform (FFT), required to compute each mode in VMD, and the linear regression contribution to eliminate eye blinks, the computational complexity of AVMD is, therefore, equivalent to $K\ \mathcal{O}(\mathcal{M}\mathcal{N}\log\mathcal{N}) + \mathcal{O}(\mathcal{N}^2+\mathcal{N}^3)$ where K, $\mathcal{M}$, and $\mathcal{N}$ are the number of modes, iterations, and samples, respectively. On the other hand, the proposed algorithm extracts only one mode for eye blink detection and uses DWT for the eye blink filtering, hence, its computational complexity is expressed as $\mathcal{O}(\mathcal{M}\mathcal{N}\log\mathcal{N}) + \mathcal{O}(\mathcal{N})$, where the first term is for the

TABLE V
CC AND RRMSE COMPARISON (MEAN±SD) BETWEEN THE EYE BLINK-FREE INTERVALS OF CONTAMINATED AND FILTERED EEG SIGNALS FOR REAL DATA

Database	VME-DWT		AVMD		DWT	
	CC	RRMSE	CC	RRMSE	CC	RRMSE
[39]	0.94±0.03	0.16±0.04	0.89±0.08	0.18±0.10	0.68±0.11	0.84±0.18
[40]	0.97±0.02	0.14±0.02	0.93±0.04	0.21±0.12	0.73±0.03	0.96±0.03
[41]	0.93±0.04	0.15±0.05	0.88±0.07	0.19±0.06	0.64±0.14	0.76±0.23
[42]	0.98±0.01	0.09±0.04	0.84±0.06	0.19±0.09	0.62±0.14	0.94±0.34

TABLE VI
THE COMPUTATIONAL TIME IN SECONDS (MEAN±SD) FOR REAL EEG DATA

Database	VME-DWT	AVMD	DWT
[39]	0.081±0.01	20.1±0.23	0.013±0.002
[40]	0.060±0.02	4.38±1.65	0.014±0.003
[41]	0.071±0.02	4.76±0.29	0.013±0.001
[42]	0.056±0.01	4.32±0.08	0.010±0.001

VME algorithm and the second term is for DWT.[3] While the required CPU time for the proposed algorithm is significantly shorter than the AVMD, DWT algorithm is advantageous over the proposed algorithm in this manner[4] (Table VI).

IV. DISCUSSION

This research proposed and evaluated the performance of the VME-DWT algorithm for the eye blink suppression in EEG signals. The obtained results suggest that the proposed VME-DWT: (a) can adequately detect and eliminate eye blinks in a short interval of single EEG channel; (b) is automatic as no human involvement is required; (c) is less invasive compared to other decomposition algorithms such as ICA, EMD, and VMD since only contaminated intervals are filtered and non-artifactual intervals remained unaltered; (d) is cost-effective as a short CPU time is required for the execution; and (e) is needless to the artifact reference and initial calibration. The proposed VME-DWT also tackles the limitations of the classical artifact detection strategies such as the amplitude thresholding and template matching as it is robust to the other high amplitude artifacts and does not require any predefined template.

While the performance of VME is not highly sensitive the value of the center frequency [28], regulation of the compactness coefficient, α, plays the key role for the accurate detection of eye blinks in EEG signals. Albeit higher value of α can guarantee extraction of the narrow-banded mode, in this application, however, smaller α values should be employed as the frequency range of eye blink violates the VME presumption by overlapping in the delta, theta and alpha bands of EEG signals [33]. This is also the plausible explanation that the extracted desired mode by VME should not be directly subtracted from the contaminated EEG signals as it would either remove some low frequency components of non-artifactual EEG or preserve some high frequency components of eye blinks. Thus, the extracted mode is used for more precise localization of the artifactual eye blink intervals. Our results suggest that $\alpha = 3000$ is the optimal value for reliable eye blink detection with the highest TPR and lowest FPR (Fig. 4 (c), (d)).

The optimal DWT decomposition level for the eye blink filtering is achieved by a skewness-based strategy between two approximation components. Such a strategy automatically terminates the decomposition procedure, evades unnecessary decomposition, and accelerates the filtering procedure. Furthermore, skewness-based strategy, unlike other wavelet-based methods [20], [34], avoids full tree decomposition of DWT or manual selection of the decomposition level. The interchangeability and effectiveness of the proposed strategy have been proven by employing contaminated EEG signals with different recording conditions.

The performance and execution time is compared to AVMD and DWT algorithms, proposed for the eye blink elimination in short intervals of a single EEG channel. In 912 semi-simulated EEG signals contaminated by eye blinks, the VME-DWT outperformed the AVMD and DWT, showing: (i) higher mean of CC values, suggesting enhanced EEG component's preservation, and (ii) lower mean of RRMSE values, showing higher filtering robustness. The denoising criteria in the frequency domain also indicate superior VME-DWT performance, especially for the preservation of low-frequency components in filtered EEG signals. In addition, VME-DWT is more robust than the AVMD and DWT in contaminated EEG signals with low SNR values. As for real data, while the proposed VME-DWT showed a satisfactory performance, the AVMD and DWT algorithm failed to attenuate the eye blinks adequately (Fig. 10). Plausible explanations for such results are twofold. Firstly, the real EEG signals used in this research could require adjustment of the parameters set for the AVMD and DWT algorithms. However, having to adjust parameters for every new database would defeat the purpose of automatization, which is, evidently, unfavorable for the real-time EEG applications. Secondly, it is plausible that the number of extracted modes or levels is insufficient, leading to the artifact markers failing to detect all eye blinks. Another advantage of the VME-DTW algorithm is its significant short

[3]It should be noted that the required computations for the initialization of center frequencies in VMD has been omitted

[4]A computer with 3.2 GHz core i7 CPU and 8 GB memory has been used to run the algorithms in MATALB 2020a environment

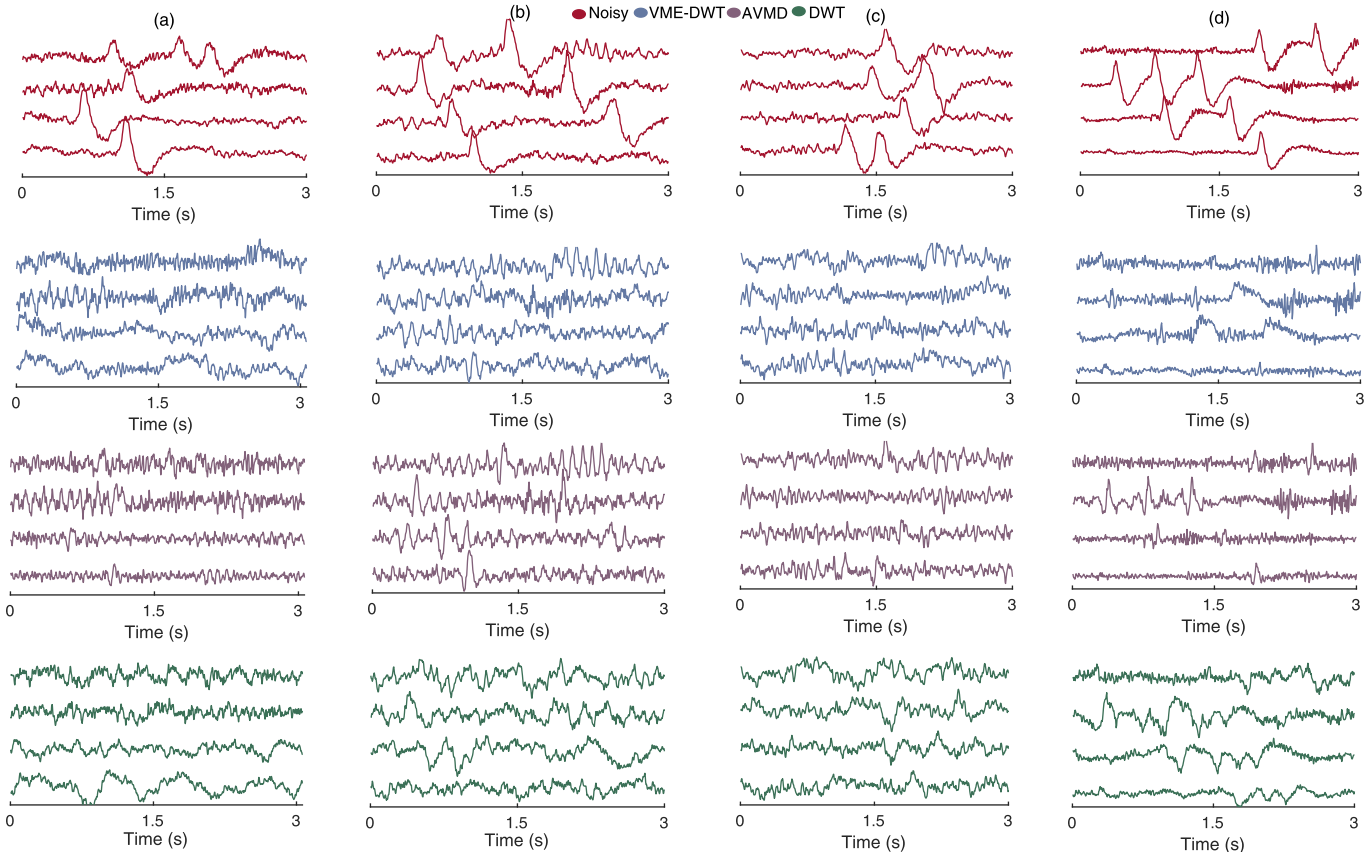

Fig. 10. Columns with examples of real contaminated EEG signal from [39] **(a)**, [40] **(b)**, [41] **(c)**, [42] **(d)**, and below the corresponding filtered EEG signals.

required CPU time, which makes it eligible for online and semi-real time applications.

While the proposed algorithm has satisfactory performance, its limitations and potential solutions should be considered. Firstly, the presence of other low-frequency artifacts such as electrode drift may hinder the accurate eye blink detection by the VME. Thus, a high-pass filter with a cut-off frequency of 0.5 Hz should be used before running the proposed algorithm. Secondly, the proposed algorithm only detects and eliminates artifacts associated with blinks, but no other artifacts such as eye saccades and muscle contractions. Nevertheless, it can be employed in conjunction with other filtering algorithms. Thirdly, this study presumes that contaminated EEG signals have only positive eye blink peaks. In bipolar EEG recordings (e.g., FT10-T8 channel), negative eye blinks might appear, and the proposed algorithm cannot detect them, unlike the AVMD and DWT. One potential solution could be to use the local minima of the extracted mode with the negative value of the threshold θ. Fourthly, while θ showed adequate performance for detection of the highest eye blink peak from VME mode, other strategies such as algebraic approach [18] or statistical threshold [19] may also improve the detection performance. Fifthly, the proposed strategy for the double eye blink event has been developed experimentally and may require further investigation for more accurate performance. Nevertheless, these suggestions to mitigate the mentioned problems are just hypothesis and require further investigation.

V. Conclusion

This paper demonstrated that VME-DWT is an efficient automatic algorithm for eye blink detection and filtering in a short segment of a single EEG channel, quantified its effectiveness and adaptiveness using semi-simulated and real world EEG data with different recording conditions, and provided insights into optimum selection of VME-DWT's parameters. According to our experimental results, the α and T values of 3000 and 0.1 can be generally used for different EEG databases. The most prominent advantage of the proposed VME-DWT algorithm is its capability to filter eye blinks in contaminated EEG signals with low SNR values, without requiring the initial calibration nor artifact reference. Besides the efficient performance, its required CPU time makes it a suitable algorithm for eye blink removal in BCI and clinical applications.

References

[1] J. W. Ahn, Y. Ku, and H. C. Kim, "A novel wearable EEG and ECG recording system for stress assessment," *Sensors*, vol. 19, no. 9, p. 1991, Apr. 2019.

[2] M. G. Bleichner and S. Debener, "Concealed, unobtrusive ear-centered EEG acquisition: CEEGrids for transparent EEG," *Frontiers Hum. Neurosci.*, vol. 11, pp. 1–14, Apr. 2017.

[3] M. Ogino and Y. Mitsukura, "Portable drowsiness detection through use of a prefrontal single-channel electroencephalogram," *Sensors*, vol. 18, no. 12, pp. 2–19, 2018.

[4] M. Ogino, S. Kanoga, M. Muto, and Y. Mitsukura, "Analysis of prefrontal single-channel EEG data for portable auditory ERP-based brain–computer interfaces," *Frontiers Hum. Neurosci.*, vol. 13, pp. 1–14, Jul. 2019.

[5] P. Gonzalez-Navarro, Y. M. Marghi, B. Azari, M. Akcakaya, and D. Erdogmus, "An event-driven AR-process model for EEG-based BCIs with rapid trial sequences," *IEEE Trans. Neural Syst. Rehabil. Eng.*, vol. 27, no. 5, pp. 798–804, May 2019.

[6] S. Narayana, R. V. Prasad, and K. Warmerdam, "Mind your thoughts: BCI using single EEG electrode," *IET Cyber-Phys. Syst., Theory Appl.*, vol. 4, no. 2, pp. 164–172, Jun. 2019.

[7] W. K. Y. So, S. W. H. Wong, J. N. Mak, and R. H. M. Chan, "An evaluation of mental workload with frontal EEG," *PLoS ONE*, vol. 12, no. 4, pp. 1–17, 2017.

[8] S.-K. Lin, Istiqomah, L.-C. Wang, C.-Y. Lin, and H. Chiueh, "An ultra-low power smart headband for real-time epileptic seizure detection," *IEEE J. Transl. Eng. Health Med.*, vol. 6, pp. 1–10, 2018.

[9] J. M. Stern, *Atlas of EEG Patterns*. Philadelphia, PA, USA: Lippincott Williams Wilkins, 2005.

[10] S. Sanei and J. A. Chambers, *EEG Signal Processing*. Hoboken, NJ, USA: Wiley, 2007.

[11] J. A. Urigüen and B. Garcia-Zapirain, "EEG artifact removal—State-of-the-art and guidelines," *J. Neural Eng*, vol. 12, pp. 1–23, Apr. 2015.

[12] A. Jafarifarmand and M. A. Badamchizadeh, "EEG artifacts handling in a real practical brain–computer interface controlled vehicle," *IEEE Trans. Neural Syst. Rehabil. Eng.*, vol. 27, no. 6, pp. 1200–1280, Jun. 2019.

[13] R. J. Barry, A. R. Clarke, S. J. Johnstone, C. A. Magee, and J. A. Rushby, "EEG differences between eyes-closed and eyes-open resting conditions," *Clin. Neurophysiol.*, vol. 118, no. 12, pp. 2765–2773, Dec. 2007.

[14] C.-Y. Chang, S.-H. Hsu, L. Pion-Tonachini, and T.-P. Jung, "Evaluation of artifact subspace reconstruction for automatic artifact components removal in multi-channel EEG recordings," *IEEE Trans. Biomed. Eng.*, vol. 67, no. 4, pp. 1114–1121, Apr. 2020.

[15] K. Jindal, R. Upadhyaya, and H. S. Singh, "Application of hybrid GLCT-PICA de-noising method in automated EEG artifact removal," *Biomed. Signal Process. Control*, vol. 60, pp. 1–16, Jul. 2020.

[16] C. Y. Sai, N. Mokhtar, H. Arof, P. Cumming, and M. Iwahashi, "Automated classification and removal of EEG artifacts with SVM and wavelet-ICA," *IEEE J. Biomed. Health Informat.*, vol. 22, no. 3, pp. 664–670, May 2018.

[17] B. Somers, T. Francart, and A. Bertrand, "A generic EEG artifact removal algorithm based on the multi-channel Wiener filter," *J. Neural Eng*, vol. 15, pp. 1–13, Feb. 2018.

[18] C. A. Majmudar and B. I. Morshed, "Autonomous OA removal in real-time from single channel EEG data on a wearable device using a hybrid algebraic-wavelet algorithm," *ACM Trans. Embedded Comput. Syst.*, vol. 16, no. 1, pp. 1–16, Nov. 2016.

[19] S. Khatun, R. Mahajan, and B. I. Morshed, "Comparative study of wavelet-based unsupervised ocular artifact removal techniques for single-channel EEG data," *IEEE J. Transl. Eng. Health Med.*, vol. 4, pp. 1–8, Mar. 2016.

[20] M. Chavez, F. Grosselin, A. Bussalb, F. De Vico Fallani, and X. Navarro-Sune, "Surrogate-based artifact removal from single-channel EEG," *IEEE Trans. Neural Syst. Rehabil. Eng.*, vol. 26, no. 3, pp. 540–550, Mar. 2018.

[21] R. Patel, M. P. Janawadkar, S. Sengottuvel, K. Gireesan, and T. S. Radhakrishnan, "Suppression of eye-blink associated artifact using single channel EEG data by combining cross-correlation with empirical mode decomposition," *IEEE Sensors J.*, vol. 16, no. 18, pp. 6947–6954, Sep. 2016.

[22] M. Saini, Payal, and U. Satija, "An effective and robust framework for ocular artifact removal from single-channel EEG signal based on variational mode decomposition," *IEEE Sensors J.*, vol. 20, no. 1, pp. 369–376, Jan. 2020.

[23] C. Dora and P. K. Biswal, "An improved algorithm for efficient ocular artifact suppression from frontal EEG electrodes using VMD," *Biocybernetics Biomed. Eng.*, vol. 40, no. 1, pp. 148–161, Jan. 2020.

[24] A. Aarabi, K. Kazemi, R. Grebe, H. A. Moghaddam, and F. Wallois, "Detection of EEG transients in neonates and older children using a system based on dynamic time-warping template matching and spatial dipole clustering," *NeuroImage*, vol. 48, no. 1, pp. 50–62, Oct. 2009.

[25] A. Klein and W. Skrandies, "A reliable statistical method to detect eyeblink-artefacts from electroencephalogram data only," *Brain Topography*, vol. 26, no. 4, pp. 558–568, Oct. 2013.

[26] W.-D. Chang, H.-S. Cha, K. Kim, and C.-H. Im, "Detection of eye blink artifacts from single prefrontal channel electroencephalogram," *Comput. Methods Programs Biomed.*, vol. 124, pp. 19–30, Feb. 2016.

[27] J. T. Valderrama, A. Torre, and B. V. Dun, "An automatic algorithm for blink-artifact suppression based on iterative template matching: Application to single channel recording of cortical auditory evoked potentials," *J. Neural Eng.*, vol. 15, pp. 1–15, Jan. 2018.

[28] M. Nazari and S. M. Sakhaei, "Variational mode extraction: A new efficient method to derive respiratory signals from ECG," *IEEE J. Biomed. Health Informat.*, vol. 22, no. 4, pp. 1059–1067, Jul. 2018.

[29] K. Dragomiretskiy and D. Zosso, "Variational mode decomposition," *IEEE Trans. Signal Process.*, vol. 62, no. 3, pp. 531–544, Nov. 2014.

[30] R. Mahajan and B. I. Morshed, "Unsupervised eye blink artifact denoising of EEG data with modified multiscale sample entropy, kurtosis, and wavelet-ICA," *IEEE J. Biomed. Health Inform.*, vol. 19, no. 1, pp. 158–165, Jun. 2014.

[31] M. E. Yablonski, *Physiology of the Eye: An Introduction to the Vegetative Functions*, 2nd ed. Boston, MA, USA: Butterworth-Heinemann, 1992.

[32] A. Bulling, J. A. Ward, H. Gellersen, and G. Tröster, "Eye movement analysis for activity recognition using electrooculography," *IEEE Trans. Pattern Anal. Mach. Intell.*, vol. 33, no. 4, pp. 741–753, Apr. 2010.

[33] S. Kanoga, M. Nakanishi, and Y. Mitsukura, "Assessing the effects of voluntary and involuntary eyeblinks in independent components of electroencephalogram," *Neurocomputing*, vol. 193, pp. 20–32, Jun. 2016.

[34] N. Mammone and F. Morabito, "Enhanced automatic wavelet independent component analysis for electroencephalographic artifact removal," *Entropy*, vol. 16, no. 12, pp. 6553–6572, Dec. 2014.

[35] N. Bajaj, J. R. Carrión, F. Bellotti, R. Berta, and A. De Gloria, "Automatic and tunable algorithm for EEG artifact removal using wavelet decomposition with applications in predictive modeling during auditory tasks," *Biomed. Signal Process. Control*, vol. 55, pp. 1–13, Jan. 2020.

[36] B. Singh and H. Wagatsuma, "Two-stage wavelet shrinkage and EEG-EOG signal contamination model to realize quantitative validations for the artifact removal from multiresource biosignals," *Biomed. Signal Process. Control*, vol. 47, pp. 96–114, Jan. 2019.

[37] J. Dammers *et al.*, "Integration of amplitude and phase statistics for complete artifact removal in independent components of neuromagnetic recordings," *IEEE. Trans. Biomed. Eng.*, vol. 55, no. 10, pp. 2353–2362, Oct. 2008.

[38] M. A. Klados and P. D. Bamidis, "A semi-simulated EEG/EOG dataset for the comparison of EOG artifact rejection techniques," *Data Brief*, vol. 8, pp. 1004–1006, Sep. 2016.

[39] H. Cho, M. Ahn, S. Ahn, M. Kwon, and S. C. Jun, "EEG datasets for motor imagery brain–computer interface," *GigaScience*, vol. 6, no. 7, Jul. 2017, Art. no. gix034.

[40] M. Kaya, M. K. Binli, E. Ozbay, H. Yanar, and Y. Mishchenko, "A large electroencephalographic motor imagery dataset for electroencephalographic brain computer interfaces," *Sci. Data*, vol. 5, no. 1, pp. 1–16, Dec. 2018.

[41] M. Torkamani-Azar, S. D. Kanik, S. Aydin, and M. Cetin, "Prediction of reaction time and vigilance variability from spatio-spectral features of resting-state EEG in a long sustained attention task," *IEEE J. Biomed. Health Informat.*, vol. 24, no. 9, pp. 2550–2558, Sep. 2020.

[42] C. Reichert, I. F. Tellez Ceja, C. M. Sweeney-Reed, H.-J. Heinze, H. Hinrichs, and S. Dürschmid, "Impact of stimulus features on the performance of a gaze-independent brain-computer interface based on covert spatial attention shifts," *Frontiers Neurosci.*, vol. 14, p. 1250, Dec. 2020.